In Vivo High-Content Evaluation of Three-Dimensional Scaffolds Biocompatibility

Mariana B. Oliveira, MSc,[1,2] Maximiano P. Ribeiro, MSc,[3,4] Sónia P. Miguel, MSc,[3] Ana I. Neto, MSc,[1,2]
Paula Coutinho, PhD,[4] Ilídio J. Correia, PhD,[3] and João F. Mano, PhD[1,2]

While developing tissue engineering strategies, inflammatory response caused by biomaterials is an unavoidable aspect to be taken into consideration, as it may be an early limiting step of tissue regeneration approaches. We demonstrate the application of flat and flexible films exhibiting patterned high-contrast wettability regions as implantable platforms for the high-content *in vivo* study of inflammatory response caused by biomaterials. Screening biomaterials by using high-throughput platforms is a powerful method to detect hit spots with promising properties and to exclude uninteresting conditions for targeted applications. High-content analysis of biomaterials has been mostly restricted to *in vitro* tests where crucial information is lost, as *in vivo* environment is highly complex. Conventional biomaterials implantation requires the use of high numbers of animals, leading to ethical questions and costly experimentation. Inflammatory response of biomaterials has also been highly neglected in high-throughput studies. We designed an array of 36 combinations of biomaterials based on an initial library of four polysaccharides. Biomaterials were dispensed onto biomimetic superhydrophobic platforms with wettable regions and processed as freeze-dried three-dimensional scaffolds with a high control of the array configuration. These chips were afterward implanted subcutaneously in Wistar rats. Lymphocyte recruitment and activated macrophages were studied on-chip, by performing immunocytochemistry in the miniaturized biomaterials after 24 h and 7 days of implantation. Histological cuts of the surrounding tissue of the implants were also analyzed. Localized and independent inflammatory responses were detected. The integration of these data with control data proved that these chips are robust platforms for the rapid screening of early-stage *in vivo* biomaterials' response.

Introduction

THE CHOICE OF BIOCOMPATIBLE MATERIALS in the development of tissue engineering strategies is crucial, as the lack of adequate immune response caused by biomaterials is one of the most common causes of failure of implants due to tissue damage and chronic response.[1,2] Although inflammatory response is commonly responsible for implants failure, it was also reported to contribute to the triggering of tissue regeneration. It is known that altered levels of tumor necrosis factor alpha (TNF-α), interleukin (IL)-1, and other proinflammatory molecules have a major effect on the healing of bone fractures.[3] Inflammation is required in neural regeneration for enhancing the proliferation of neural progenitors and neurogenesis,[4] and it has also a necessary involvement in the salamanders' limb regeneration, a process dependent on the presence of macrophages.[5]

Regeneration using mesenchymal stem cells was also proven to be dependent on recipient T lymphocytes, through the interferon gamma-induced downregulation of Runx-2 and enhancement of TNF-α signaling in cells.[6] To discover optimized formulations of biomaterials for tissue regeneration, it is important to screen different and high numbers of combinations of materials. In this complex process, one of the key aspects to take into consideration is the inflammatory response caused by such materials, and its role in implant rejection or as regeneration adjuvants.

High-content approaches to study cell–biomaterial interactions have allowed collecting large amounts of data about single and combined molecular interactions affecting tissue regeneration. The ultimate goal of these approaches is to perform assays in a resource- and time-saving manner.[7–9] Biomaterials with beneficial properties for stem cells culture[10–15] and bacterial attachment prevention[16] were spotted

[1]3B's Research Group—Biomaterials, Biodegradables and Biomimetics, University of Minho, Headquarters of the European Institute of Excellence on Tissue Engineering and Regenerative Medicine, Taipas, Portugal.
[2]ICVS/3B's—PT Government Associate Laboratory, Braga/Guimarães, Portugal.
[3]CICS-UBI—Health Sciences Research Center, Faculty of Health Sciences, University of Beira Interior, Covilhã, Portugal.
[4]UDI-IPG—Research Unit for Inland Development, Polytechnic Institute of Guarda, Guarda, Portugal.

using microarray methods.[17] Over time arrayed platforms for high-content studies matured from platforms that allowed studying cell-2D material interactions to platforms compatible with cell encapsulation in hydrogels, allowing for a closer *in vivo*-like approach. These studies were carried out in *in vitro* environment. As such, information was lost on inflammatory response of these materials, as well as other phenomena resulting from the complexity of the *in vivo* environment. The lack of established methods for *in vivo* combinatorial analysis led us to develop the method described herein.

Hereby, we propose the implantation of superhydrophobic flexible and flat platforms with patterned arrays of wettable regions where combinations of biomaterials are dispensed and processed as independent porous scaffolds. These chips are used to study foreign body response in localized spots in a high-throughput manner.[18–20] Similar platforms were used *in vitro* for the study of protein–cell interactions in two-dimensional (2D) environment, cell-laden three-dimensional (3D) hydrogels, and 3D scaffolds.[19–21] We hypothesize that the miniaturized size of the patterned biomaterials and the gap maintained between them would be sufficient to observe distinct inflammatory cells recruitment while allowing for isolated responses in each spot. Moreover, the low cell adhesion reported in superhydrophobic surfaces would improve the independency between spots.[18,22] For the proof-of-concept, we designed an array of 36 combinations of biomaterials from a small library of four materials: chitosan (Chi), alginate (Alg), and two carrageenans: k-carrageenan (k-Carr) and ι-carrageenan (ι-Carr), the latter having a higher number of sulfate groups. We aimed to study the effect of distinct anionic surfaces combined with Chi, as they were reported to promote higher levels of macrophages and adherent lymphocytes, compared to materials with distinct chemical features.[23] The individual inflammatory response of Chi[24] and Alg[25] applied as biomaterials was previously investigated. For carrageenans, inflammatory response in the form of implantable biomaterials is still poorly described. However, carrageenan solutions with high number of sulfate groups (ι-Carr and λ-carrageenan) are widely used to trigger inflammation for *in vivo* studies.[26] Our proposed methodology has the potential to be adapted to diversified combinations of biomaterials, allowing saving high numbers of animals. The direct application of the method would result in an important ethical achievement, along with the consequent optimization of costs adjacent to animal experimentation.

Materials and Methods

Superhydrophobic surfaces with wettable transparent spots

Polystyrene films (ST311190; Goodfellow) were cut into 4×4 cm^2 squares. 6×6 arrays of polyvinyl stickers (Oracal) were patterned in the surfaces. The arrays were constituted by squares of 4 mm^2, separated by 2 mm in all sides (Fig. 1). The surfaces were treated by a phase-separation method, as described elsewhere.[27] Briefly, a solution of commercial grade polystyrene in THF (Sigma) (70 mg mL^{-1}) and ethanol absolute (in proportions of 2:1.3) was poured onto the polystyrene films. The solution was then removed and the surfaces were immersed in ethanol absolute. After 1 min under immersion, the surfaces were let to dry at room temperature. The stickers were then totally removed and the

whole surface washed with pure ethanol to remove possible traces of the stickers' glue. The chips were afterward cut into four geometrically equal squares with nine biomaterials per square (3×3 array) for implantation.

Biomaterials array deposition

Our experimental design consisted of a matrix of 36 combinations of biomaterials. The processing of biomaterials followed two steps: first, we prepared freeze-dried genipin-crosslinked scaffolds, with distinct concentrations of Chi ("A," in Fig. 2D, E) in acetic acid (2% v/v) solution: 1%, 1.5%, and 2% (w/v). We previously proved that these Chi concentrations are adequate for the preparation of porous scaffolds on such chips.[21] Nine scaffolds of each concentration were prepared in the chips (Fig. 2D). After freeze-drying the Chi structures, solutions of other polymers (labeled "polymer B") were dispensed on the top of these porous scaffolds in distinct concentrations (Fig. 2E).

Medium-molecular-weight Chi (ref. 448877, batch MKBJ9698V; Sigma), with 75% to 85% of desacetylation, was purified according to a reprecipitation method. A solution of crosslinker was prepared with 4% (w/v) genipin (Comercial Rafer, S.L.) in distilled water and ethanol (90:10 v/v). The Chi scaffolds were prepared by pipetting 4 μL of Chi solutions and 2 μL of genipin in each wettable spot of the chip. One additional condition of 1.5% (w/v) of Chi was added to the array, where the volume of Chi dispensed in the wettable regions was 6 μL. This condition is referred as "1.5% +." Crosslinking occurred at 37°C in water saturated environment. Afterward, the chips were frozen at -20°C for 2 h and -80°C overnight. Freeze drying occurred at -80°C, 0.3 bar. Polymers B (Fig. 2E) were added afterward to the Chi freeze-dried scaffolds in amounts of 2 μL. Polymers B were Alg (ref. W201502; Sigma), k-Carr (ref. 22048; Sigma), and ι-Carr (ref. 22045; Sigma), in concentrations of 2% (H), 1% (M), and 0.5% (L) (w/v). They were used as received. They were crosslinked with KCl for k-Carr (JMGS) or CaCl$_2$ (VWR) for ι-Carr and Alg, both at concentration 1M. The chips were again frozen at -20°C for 2 h and -80°C overnight. Freeze-drying occurred at -80°C, 0.03 bar.

Control samples

On-chip controls. On-chip control samples were processed in an equivalent manner to the standard chips. Biomaterials were dispensed in a randomized configuration, indicated in Supplementary Table S1 (Supplementary Data are available online at www.liebertpub.com/tec).

Implantable plugs. Two random conditions were selected from the array of biomaterials: Chi 1% ι-Carr 2%H and Chi 1% Alg 2%H. Plugs with 5 mm diameter × 3 mm height of these conditions were processed in commercially available 96-well plates. A volume of 200 μL of Chi solutions was dropped in each well, followed by 100 μL of genipin solution, in the same proportions and concentrations used for on-chip experiments. The well plate was then placed at 37°C for 3 h, while the crosslinking reaction took place. The samples were then frozen and freeze-dried, in the same conditions as the on-chip ones. The solutions of polymer B were dispensed on the top of the previously
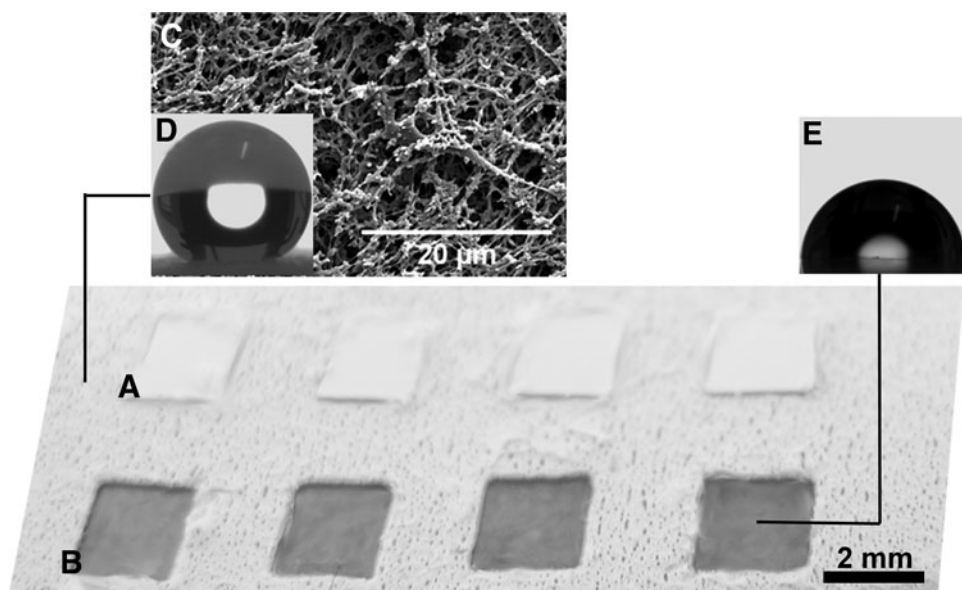
FIG. 1. Image of a part of an array of patterns on the chip with (**A**) protective stickers and (**B**) after removing the protective stickers, with transparent wettable spots. (**C**) Scanning electron microscopy image of superhydrophobic domain of the chip. (**D**) Representative profile of a water droplet on the superhydrophobic domain of the chip (contact angle of $156.2° \pm 0.3°$). (**E**) Representative profile of water droplet on the non-treated part of the chip—wettable region (contact angle of $90.5° \pm 4.7°$).

prepared Chi sponges according to the proportions used on-chip and then crosslinked with 50 μL of the crosslinking solutions. Freeze-drying was repeated. The samples were washed and sterilized using the same procedure of on-chip samples.

Sterilization of the chips and control plugs. The chips with the scaffolds in their final stage of processing were immersed in ethanol 70% (Panreac) for 30 min. Before implantation, they were washed with sterile physiological buffer solution (PBS; Fluka) for 15 min, three times. The same procedure was performed for the plugs implants prepared without the superhydrophobic film and to the empty chips.

Implantation of the chips and control samples in Wistar rats

The 36 spot chips were cut in 4 parts (with 9 miniaturized scaffolds per part), the chips boarders were cut with rounded shape as close to the scaffolds as possible, and a mark was made on each chip, to identify the relative position of the biomaterials after explantation. The chips were then implanted subcutaneously in Wistar rats for 24 h and 7 days with the configuration indicated in Figure 2D and E.

To perform the *in vivo* assays, a total of 27 Wistar rats (8–10 weeks old), weighing between 150–200 g, were used. The project was conducted in accordance with the international guidelines set for animal research. This study was conducted in the animal research facility of the University
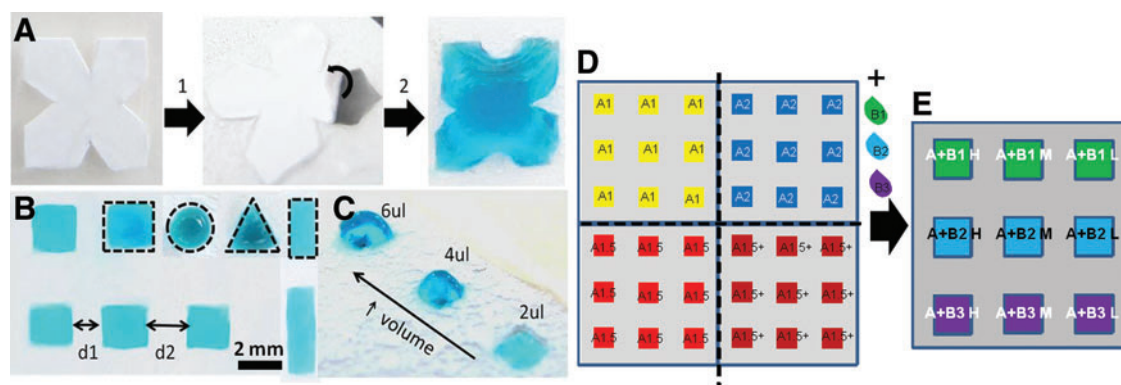

FIG. 2. (**A**) Preparation of superhydrophobic patterned chips using removable stickers (**B**) allowing to imprint complex geometrical wettable features surrounded by superhydrophobic domains (step 1 refers to the stickers in the polystyrene-untreated film; step 2 shows the superhydrophobic polystyrene chip where the protecting sticker is being removed so the wettable area is exposed). Liquid precursors can be dispensed in wettable regions with distinct sizes and shapes (**B**) (see examples delimited by dashed lines) and with different volumes (**C**). (**D**) Setup used to prepare the implanted chips, where Chi (''A'') was patterned in distinct concentrations (1%, 1.5%, 2%, and 1.5 + %) and separated by different distances (d1, d2), as described in the Results section. (**E**) Biomaterials (''B'') were added to the previously freeze-dried Chi scaffolds in distinct dilutions (H, M, and L for lower, medium, and highest dilution factor of polymer ''B''), to obtain chips with distinct combinations of biomaterials. The implanted chips with 9 scaffolds were cut from the previous chip with 36 scaffolds. Chi, chitosan. Color images available online at www.liebertpub.com/tec

of Beira Interior. Housing and animal care were provided according to procedures set for animal research. Animals were individually anesthetized with an intraperitoneal injection of ketamine ($40\,mg\,kg^{-1}$) and xylazine ($5\,mg\,kg^{-1}$). Subsequently, each animal was immobilized and the dorsum was shaved, washed, and disinfected with ethanol (96%). To perform chip implantation, a 1.5- to 2-cm skin incision was done in four different sites of animal dorsum (Fig. 3A). The animals were divided in several groups. The first group corresponded to animals where the 4 different chips (with Chi in the different concentration: 1%, 1.5%, 2%, and 1.5+%) were implanted ($n \geq 4$). All biomaterials faced the muscle side of the cut. Four chips with random configuration of the spotted biomaterials (as indicated in Supplementary Table S1) were implanted in rats ($n = 3$). The second group was similar to the first group; however, in these animals, the chip with the condition ''1.5+%'' was substituted by a chip without any spotted biomaterials (empty chip) ($n = 2$). Control groups were set as one group with two empty chips implanted ($n = 2$). One biomaterial plug was implanted by animal ($n = 2$) to be explanted after 24 h and 7 days of implantation. Subsequently to samples implantation, the skin flaps were sutured. During the study, animals were kept in separate cages and fed with commercial rat food and water *ad libitum*. Animals were sacrificed by CO_2 asphyxiation after 24 h and 7 days.

Immunocytochemistry

After the explants of the 4 chips in each animal, the chips were fixed and kept in paraformaldehyde (Fig. 3E). The explanted chips were incubated with primary antibodies CD25 (AbD Serotec) (specific for IL-2 produced by lymphocytes) or CD163 (AbD Serotec) (specific for macrophages) in concentration of 1:100 overnight, at 4°C. Nonspecific binding was blocked by incubation with 3% bovine serum albumin (BSA) solution in PBS for 30 min, at room temperature. After 1 h of incubation with Alexa-Fluor488 (Alfagene) for CD25, or AlexaFluor594 (Alfagene) for CD163, both at a concentration of 1:250, in BSA 1%, at room temperature, the cells were washed in PBS and counterstained with DAPI (Invitrogen) nuclear staining. The presence of surface markers was analyzed using an Axioplan Imager Z1 fluorescence microscope (Zeiss). Images in a total height of $500\,\mu m$ were acquired in 20 layers of

$25\,\mu m$. The images used for the analysis were the ones corresponding to the final stacking of the 20 layers.

Histological analysis

Tissue specimens were obtained from the implantation area by sharp dissection at 24 h and 7 days and then fixed with paraformaldehyde and paraffin embedded. To obtain a full analysis of all materials present in the chips, different perpendicular sections to the chip were obtained from the tissue in contact with different samples. Histological cuts were performed in the first 2 mm of the tissue in contact with the chip, followed by 4 mm cuts. A 3-μm section obtained from each paraffin block was stained with hematoxylin and eosin.

Lymphocytes quantification

Images acquired by microscopy (Axiovision; Zeiss) with a $50\times$ magnification were cut into four equal images. Using ImageJ (NIH) software, the background caused by the natural fluorescence of natural polymer in each image was removed or minimized. Automatic nuclei counter (ITCN, ImageJ; NIH) was used to quantify the lymphocytes. Images with the green staining were analyzed considering cells with $6\,\mu m$ of diameter and a separation dependent on the density of cells, varying from 2 to $6\,\mu m$. Representative images of the steps performed for the cell quantification can be consulted in Supplementary Figure S1.

Score attribution for histological cuts and macrophages immunocytochemistry

For histological sections, scoring was attributed to each part of the histological cuts (divided according to Fig. 3C) according to the following scale: 0—absence of inflammatory cells; 1—presence of lymphocytes and polymorphonuclear (PMN) cells; 2—higher presence of lymphocytes and PMN, and low amount of macrophages; 3—higher presence of lymphocytes; 4—high concentration of macrophages and presence of lymphocytes; 5—very high density of macrophages; 6—vascularization with very high concentration of macrophages. Images of on-chip macrophages were scored (0–6) according to the relative amount of macrophages in the scaffold, where 0 corresponded to the lowest relative amount and 6 to the highest relative amount.
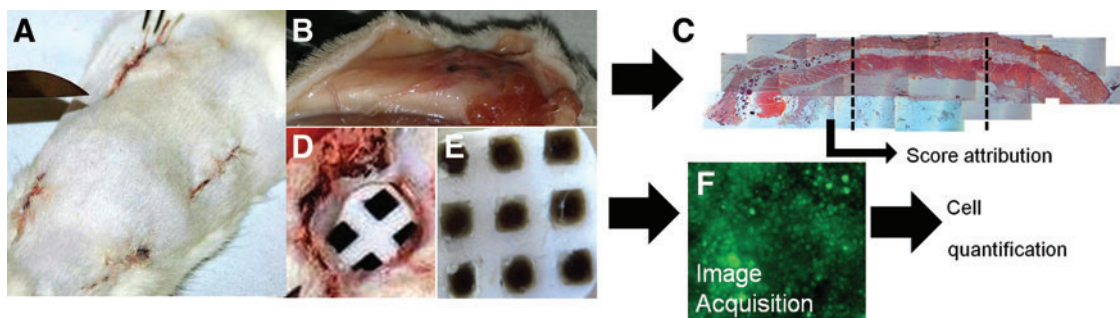

FIG. 3. **(A)** Dorsal view of an animal after the implantation of the four chips in the used configuration. **(B)** Tissue surrounding the chip after 7 days of implantation. **(C)** Example of a histological cut performed to explanted tissue around the chip. **(D)** Removal of one chip after 1 day of implantation. **(E)** Explanted chip after 24 h of implantation. **(F)** Image of immunocytochemistry performed to lymphocytes in one of the conditions of the chip after 24 h of implantation. Color images available online at www.liebertpub.com/tec

Generation of intensity maps

The color attributed to each spot of the intensity maps corresponded to the average values of the studied variables (e.g., quantified cell number or attributed score). Numerical values and respective standard deviations can be consulted in Supplementary Figures S2–S7. The colors of the intensity maps were generated with Microsoft Office Excel (Microsoft®) according to the following criteria: lower value corresponded to turquoise blue and higher value to bright red. The middle color was allocated to the 50% value of the distribution of the maximum and minimum values registered in the groups of values analyzed. This attribution was performed according to the groups of results presented in the same figure or section of figures.

Factorial analysis

Exploratory factor analysis is a technique within factor analysis statistic methods used to uncover the underlying structure of sets of variables. Three-factor analysis was performed using the Design of Experiments DesignExpert7 Software (Stat-Ease, Inc.). Response surface models were generated for the analyzed conditions and the contribution of each factor was then quantified. The three factors considered were: concentration of Chi in the scaffold (% Chi, factor A), type of polymer "B" (polymer, factor B), and dilution of polymer B (dilution, factor C). The variables were considered as numerical, for factor A and factor C, and nominal for factor B. Three levels were considered for factor A: 1%, 1.5%, and 2%. Three levels were considered for factor B: Alg, k-Carr, and ι-Carr. Factor C was analyzed also considering three levels: H—for lower dilution factor (i.e., higher concentration of polymer B: 2%), M—for intermediate dilution factor (concentration of polymer B: 1%), and L—for higher dilution factor (concentration of polymer B: 0.5%). For histology scores analysis, the Chi concentration 1.5% was isolated, so a three-factor analysis was performed considering a new factor: the volume of Chi dispensed (factor D): 4 (1.5% Chi) or 6 μL (1.5% + Chi).

We developed three distinct surface response models for each time point: 24 h and 7 days after implantation. Each model was developed according to the quantified number of lymphocytes, scores attributed to on-chip macrophages, and to each part of the histological cuts performed in the tissue collected around the chips. The results were analyzed by the software by "sequential model sum of squares" to select the highest order polynomial where terms were significant and the results were not aliased. For most of the models, response surface 2FI models were suggested and furtheron generated. For lymphocyte and macrophage quantifications after 24 h of implantation, main effect models were generated. Results were then analyzed by analysis of variance (ANOVA). Each model allowed concluding about the percentage contribution of each factor. The effect of each factor and the combined effect of factors were also analyzed.

Statistical analysis

Two-way ANOVA with Bonferroni post-test was performed to obtain the results of standard chips (main experiment), resulting from the implantation in the first group of animals, considering the results of lymphocyte quantification and scoring of macrophages on-chip, as well as of histology images. Three distinct variables were considered: effect of polymer B, effect of dilution of polymer B, and effect of Chi concentration. The results of significant differences can be consulted in Supplementary Table S2.

Results and Discussion

We implanted 36 miniaturized combinations of biomaterials in single animals using chips based on extreme water repellency (Figs. 1–3) with patterned arrays of wettable regions (Figs. 1 and 2A–E) where combinations of biomaterials (Fig. 2D, E) were dispensed and processed as independent porous scaffolds (Fig. 3E). The chips are versatile, allowing patterning a high diversity of shapes, sizes (Fig. 2A, B), and amounts of biomaterials (Fig. 2C), processed by several techniques and with the possibility of showing anisotropic features and distinct and geometrical configurations between them (Fig. 2B). These chips—where the surface of biomaterials is totally exposed to the *in vivo* environment (Fig. 3E)—were used to study foreign body response in localized spots in a high-throughput manner. The liquid biomaterial precursors were strongly restricted in the wettable regions due to the high-contrast of surface tensions (Fig. 2A–C).[18–20] Superhydrophobic surfaces prepared by phase separation methods showed low cell adhesion,[18] including substrates prepared using polystyrene.[22] Therefore, we expect that the scaffold spots could be maintained relatively isolated from each other, avoiding cell passage between spots and minimizing the interaction of the platform with the *in vivo* milieu.

All biomaterials patterned in the chips remained attached to the wettable regions of the chip after 24 h of implantation (an example of an explanted chip can be observed in Fig. 3E). After 7 days of implantation, a small percentage of the scaffolds was integrated in the animals muscle, as the majority of the scaffolds remained attached to the chip. The response to biomaterials that remained attached to the chip was studied by immunocytochemistry along with the histological cuts performed in tissue surrounding the chip.

From here on, the set of polymers added to the Chi scaffolds—Alg, k-Carr, or ι-Carr—will be labeled as polymer B, and the dilution of such polymers will be indicated as H (indicating the lowest dilution; 2% w/v polymer concentration), M (indicating an intermediate dilution; 1% w/v polymer concentration), and L (indicating the highest dilution; 0.5% w/v polymer concentration).

Analysis of on-chip immunocytochemistry

After being explanted, scaffolds were analyzed on-chip by immunocytochemistry, for the presence of both lymphocytes and macrophages. The lymphocytes were labeled with a green secondary antibody and macrophages with a red one. Figure 4 depicts representative examples of fluorescence microscopy performed to the chips where the presence of both cell types can be seen after 24 h and 7 days of implantation. Figure 5 depicts the representative histological cuts surrounding the biomaterials, which were analyzed complementarily with the on-chip biomaterials. Lymphocytes present on each formulation were quantified by image analysis using ImageJ software; the procedure is explained in Supplementary Figure S1. The presence of macrophages in each formulation was evaluated according
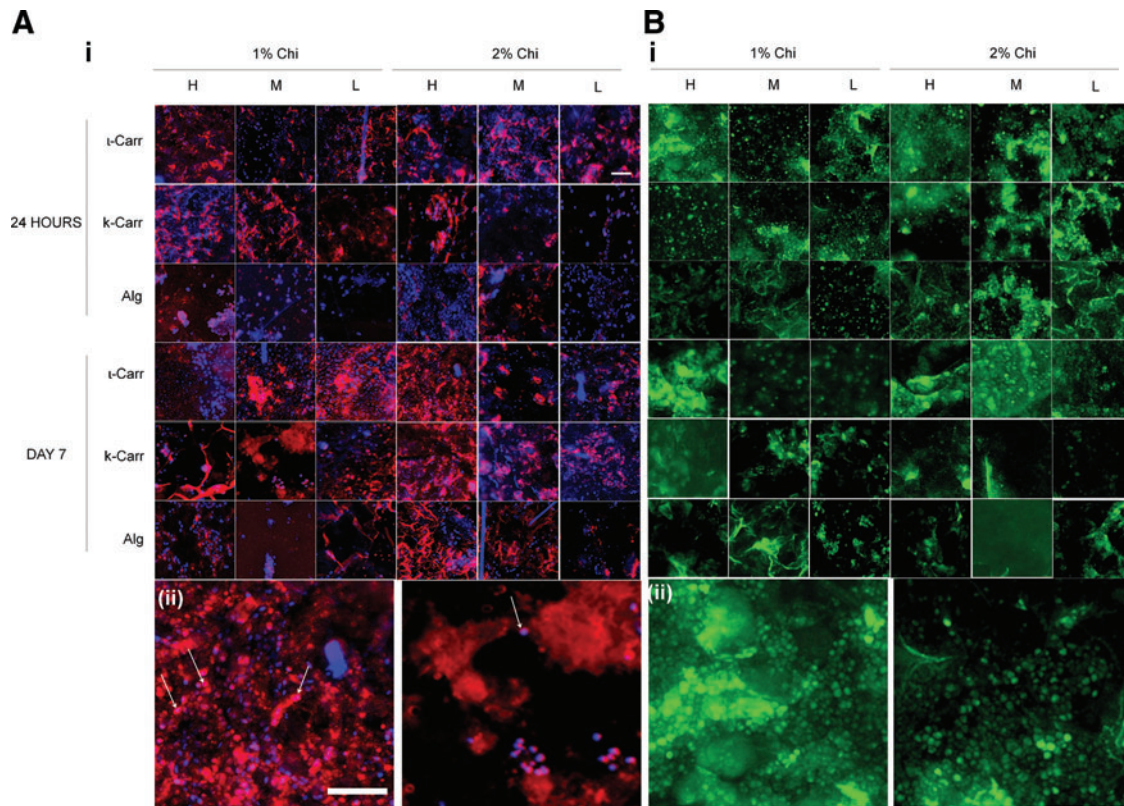
FIG. 4. **(A) i:** Immunocytochemistry pictures of macrophages (in red) in each scaffold of the chips. **ii:** Magnified pictures of conditions D1 1% Chi ι-Carr H (left) and D1 1% Chi k-Carr L (right) where the morphology of the lymphocytes can be observed. **(B) i:** Immunocytochemistry pictures of lymphocytes (in green) and staining of the nucleus (DAPI, in blue) present in each scaffold of the chips. **ii:** Magnified pictures of conditions D7 2% Chi ι-Carr H (left) and D7 1% Chi k-Carr M (right), where the morphology of the macrophages can be observed. Some macrophages are indicated with white arrows. Scale bar = 50 μm. k-Carr, k-carrageenan; ι-Carr, ι-carrageenan. Color images available online at www.liebertpub.com/tec

to a score explained previously in the Materials and Methods section. After the quantification of lymphocytes and score attribution to macrophages presence in each condition, an intensity map was built (Fig. 6). By color analysis of the maps in Figure 6, all conditions on-chip can be rapidly compared in terms of average mean values obtained for lymphocytes quantification and macrophages scores. The numerical values with respective standard deviations can be found in Supplementary Figures S2–S7. Further on, the results will also be reported and discussed taking into consideration the statistical analysis of such results. Both on-chip data and histological sections results were analyzed with two-way ANOVA with Bonferroni post-test. For the on-chip data obtained from the quantification of immunocytochemistry images, analysis was performed to all combinations of the ionic networks with both 1% Chi and 2% Chi. All conditions from the histological examination were analyzed for statistical significance (results in Supplementary Table S2).

After 24 h of implantation, the presence of lymphocytes in the scaffolds was very similar in all conditions containing ι-Carr; no significant differences were observed between any of these conditions. The effect of dilution factor of polymer B was observed between H and M, H and L, as well as M and L, mainly for Alg-containing conditions, where L led to lower lymphocytes number than M, and those to lower scores than H conditions. Conditions containing ι-Carr were significantly different from both conditions

containing k-Carr and Alg, and k-Carr conditions were different from those containing Alg. ι-Carr conditions showed higher lymphocytes numbers, followed by k-Carr and Alg. For k-Carr- and Alg-containing conditions, significant differences were registered with 1% Chi and 2% Chi. Higher concentration of Chi (2%) was responsible for higher concentration of lymphocytes. Lymphocytes have been shown to adhere to surfaces *in vitro*.[28] In lymphocyte/macrophage cocultures, lymphocytes have been observed to associate with macrophages and foreign body giant cells.[1] Regarding the presence of macrophages in the biomaterials after 24 h of implantation, no significant differences were observed between the conditions.

We observed a transient presence of lymphocytes after 24 h of implantation. The evolution of inflammatory response until day 7 was also monitored by analysis of different inflammatory cells present in the distinct biomaterials. Lymphocytes registered a transition from 24 h to 7 days: their amount decreased significantly in all conditions, mainly in the ones containing Alg, where their presence was almost inexistent (Fig. 6A). Their presence was also very low in k-Carr-containing conditions. Increasing concentrations of Chi in the substrate scaffold led to higher number of lymphocytes attached to the biomaterials, namely in the 2% k-Carr condition and in ι-Carr conditions. We also observed that the lymphocytes withdrawal gave place to the increase of macrophages in the biomaterial. Lymphocytes
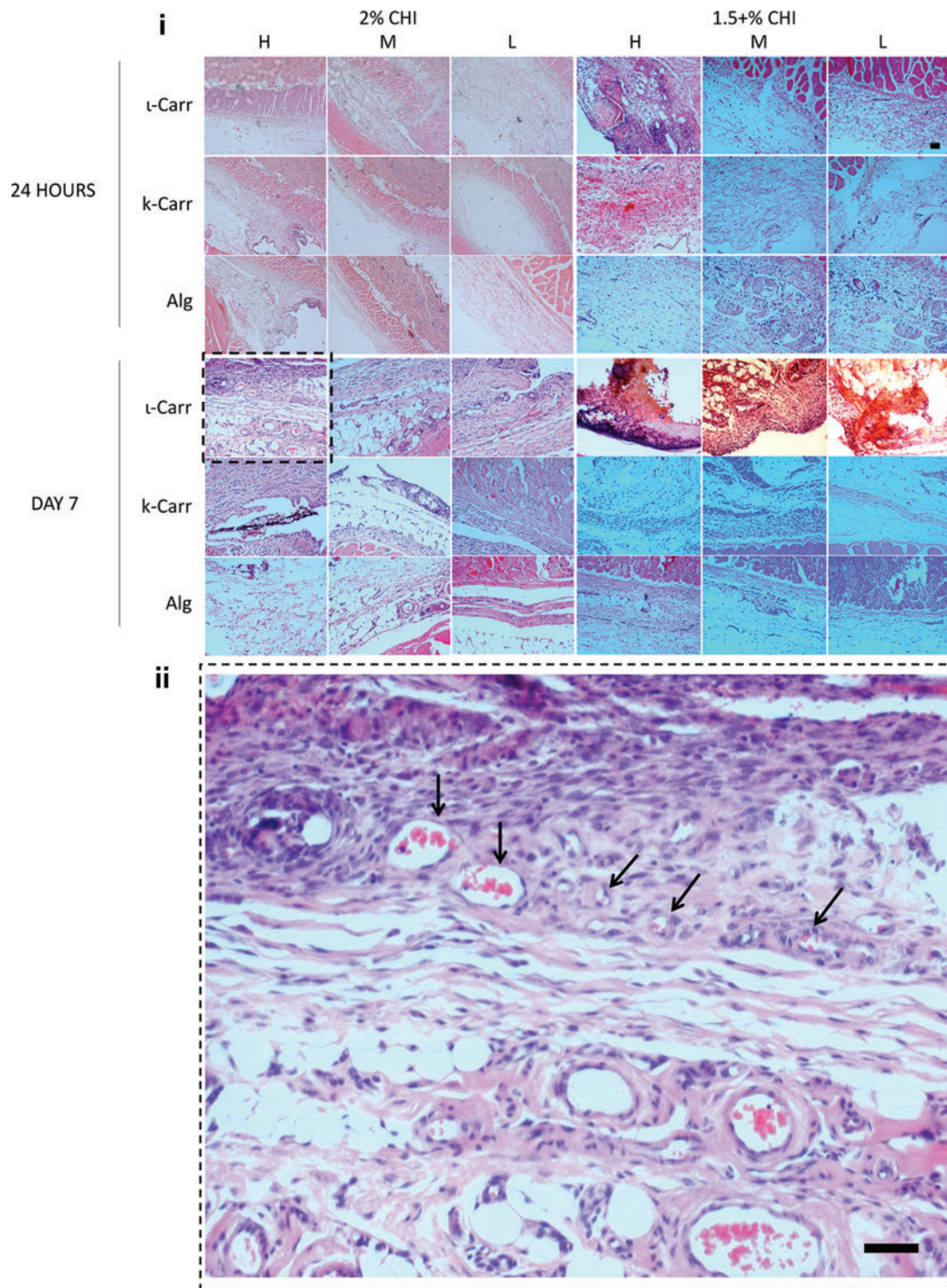
FIG. 5. **i:** Pictures of histological sections of 2% Chi and 1.5% + Chi conditions. **ii:** Magnification of the condition 2% ι-Carr in 2% Chi scaffold (image framed in **i**). The presence of higher amount of blood vessels (indicated by black arrows) can be observed in this condition. Scale bars = 50 μm. The nomenclatures H, M, and L correspond to high, medium, and low dilution factors of polymer B, respectively. More detailed information on cell type identification can be observed in Figure 9. Color images available online at www.liebertpub.com/tec

were previously reported to be transiently present at the implant site.[23] They have been shown to interact with monocytes and macrophages resulting in mutual effects on each other in terms of activation and enhanced inflammatory responses. The conditions with more concentration of macrophages were the ones with k-Carr and ι-Carr. These results were consistent with the dilution of polymer B present in the combinatorial biomaterials, since H and M materials showed higher amount of macrophages than those with dilution factor L.

Analysis of histological cuts

After collecting the chips from the animals, the tissue that surrounded each chip was also collected for histological analysis. The analysis of the tissues was performed by the attribution of histological scores to three different parts of the histological cuts (performed in the tissue perpendicularly to the chip position during implantation), exemplified in Figure 3C. Figure 5 shows representative images of the parts of the histological parts that were in contact/closer to each biomaterial patterned on the chips. The scoring scale is explained in the Materials and Methods section. An intensity map with colors corresponding to the ranking of the average values attributed to each region of the histological cuts can be observed in Figure 5B. Average scores values, standard deviations, and significant differences between all conditions can be found in Supplementary Figs. S2 and S3 and Supplementary Table S2.

According to the general tendencies observed in Figure 6B, after 24 h of implantation, higher histology scores were attributed to the conditions containing ι-Carr and k-Carr when compared to the ones containing Alg. Biomaterial conditions with lower dilution factor (H) were significantly different between ι-Carr and Alg, and k-Carr and Alg. We did not observe any significant differences between biomaterials containing ι-Carr and k-Carr. The increase of dilution factors of the polymer B (from H to L) led to a decrease in the general tendencies of histology scores in all conditions, regardless of polymer B. The majority of statistical differences were observed while comparing H with L dilution factors. Conditions containing k-Carr as polymer B were the ones more sensitive to changes in the dilution factor from H to M (intermediate dilution factor) and M to L. The presence of distinct polymers B in the biomaterials combinations also led to differences in the histology scores, namely in the H dilution condition. Statistical differences were found between biomaterials containing ι-Carr/k-Carr and biomaterials containing Alg. No statistical differences between materials with ι-Carr and k-Carr were observed.

After 7 days of implantation, significant differences between H and M dilution factors were observed in biomaterials containing ι-Carr. Materials with M dilution factor were attributed with lower histological scores. No other correlations between the dilution factors were observed. In several dilution conditions and Chi concentration biomaterials containing ι-Carr were attributed with higher scores than the ones with k-Carr and Alg. No statistically relevant differences between materials containing k-Carr or Alg were found.

Factorial analysis

We developed three distinct factorial analysis models for each time point: 24 h and 7 days after implantation. Each model was developed according to the quantified number of lymphocytes (obtained from microscopy images as the ones represented in Fig. 4B), scores attributed to macrophages analyzed on-chip (attributed to microscopy images as the ones represented in Fig. 4A), or to the histological scores attributed to each part of the histological cuts (as the ones represented in Fig. 5) performed to the tissue collected around the chips. The analysis was performed considering the average values for each of these parameters (as represented in Fig. 6). Each model allowed concluding about the percentage contribution of each factor affecting the results. For the models generated from the data collected on 24 h time point, histology scores allowed obtaining a robust surface response model (with 99.9% of confidence), where not only the main effects but the effect of interacting factors could be analyzed. The contribution of each factor and interactions between factors for each time point can be seen in Figure 7.

For lymphocyte and macrophage analyses after 24 h of implantation, the model was not significant to analyze the effects of combined factors, so a model analyzing only the main effects was applied. For the case of histological scores, all individual factors contributed significantly to the variation of inflammatory phenomena. The main effect contributing was the dilution of polymer B (factor C, in Fig. 7), with 63% of contribution, followed by the type of polymer B (factor B), with 17% of contribution. Regarding the analysis of lymphocytes after 24 h of implantation, the only factor considered
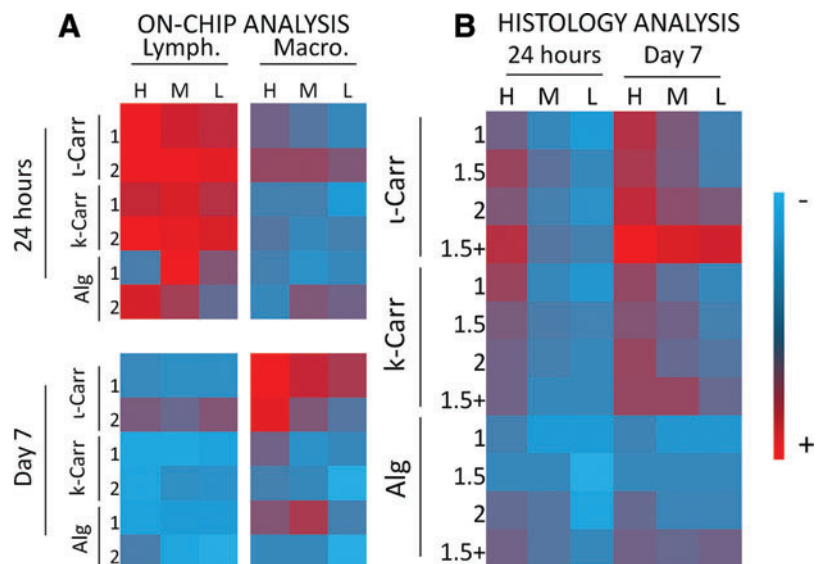

FIG. 6. Intensity map, according to the color gradient (right), with colors attributed to average values obtained for (**A**) the quantification of lymphocytes (Lymph.), macrophages (Macro.) and (**B**) for scores attributed to histological analysis, after 24 h and 7 days of implantation. Color images available online at www.liebertpub.com/tec

FIG. 7. Contribution of the effect (%) of each factor and combination of factors in the surface response models. Data to generate the surface response models was obtained for lymphocyte, macrophage, and histological scores evaluation with distinct biomaterials after 24 h and 7 days of implantation. **(A)** Models considering factor A as % Chi and **(B)** models considering factor A as volume of Chi for the 1.5% and 1.5 + % conditions. Significant effects are labeled with "*." The total value of the addition of factor contribution is not 100%, as the values attributed to residues of the model are not shown herein. Color images available online at www.liebertpub.com/tec

relevant to the results was the type of polymer B present in the biomaterials. For macrophage scores, both percentage of Chi (factor A) and type of polymer B (factor B) were considered significant for the surface response model.

After 7 days of implantation, data obtained both from on-chip and histological scores analysis allowed obtaining robust models, with 99.9% of confidence. All individual factors showed a significant effect in the histological scores attributed to the distinct biomaterials. The individual factor with more relevance was the dilution of polymer B (factor C), with 48% of contribution to the model. The effect of Chi percentage of the substrate porous scaffold (factor A) contributed with 6%, and the dilution of polymer B (factor B), with 34%. Moreover, BC interactions were also considered as statistically relevant, although with less impact than individual factors. Regarding on-chip analysis, lymphocytes number was affected mainly by factors A (27%) and B (46%), whereas macrophages score was affected by factors B (48%) and C (31%).

Regarding the factorial analysis performed to the histological scores of conditions 1.5% Chi and 1.5% + Chi—which is a condition where the scaffolds were not prepared from 4 μL volume of Chi, but from a higher volume of 6 μL—(Fig. 7B), the main effects affecting the inflammatory response observed after 24 h of implantation were the type of polymer B (with 21% of contribution) and the dilution of polymer B (with 55% of contribution). In this time point, all factors and combined effects were statistically relevant for the scores attributed. After 7 days of implantation, the main effects contributing to the attributed scores of the histology images were the type of polymer B in the biomaterials (43%), as well as the volume of Chi (factor D) used in the Chi scaffold (32%). Except for the interaction DC, all factors and combined effects were significantly relevant for the developed surface response model.

Correlation between on-chip and histology results

For 24 h of implantation, the results obtained for on-chip analysis and histology analysis were not directly correlated. This may be explained by the lack of robustness of the models obtained for on-chip cell analysis (for macrophages analysis, a low value for predicted $R^2 - 0.20$—was obtained). Moreover, after 24 h of implantation, cells involved

in inflammatory response may have not reached the material, and may still be migrating to the materials. Histology showed that, in fact, lymphocytes along with PMN and some macrophages were present in the tissue around the biomaterials (Fig. 5).

After 7 days of implantation, the effect of the factors on-chip and obtained from the analysis of histological scores were easily correlated (Fig. 7). The effects obtained for the histological analysis were similar to the combined analysis of the effect of both lymphocytes and macrophages. Therefore, after 7 days of implantation, the results can probably be directly obtained from on-chip image-based methods, without the loss of any important information. This is an important outcome of the method that permits assessing information on biomaterial–tissue interaction in a high-throughput form, without the need of time-consuming histology analysis.

General analysis of biomaterials'
inflammatory response

Regarding the general response from the explanted chips, no fibrotic capsule or macroscopic signs of inflammation were observed (Fig. 3D). The histology analysis performed to the tissue around the chips (Fig. 10C) suggests that the reaction observed in each chip is totally independent between the four implanted chips. Moreover, animals showed a normal behavior during the implantation period (Supplementary Video S1).

Chi crosslinked with genipin was used as the base material for all biomaterials studied in this approach. Chi inflammatory response was previously described for the mice model.[29] In this work, histological assessment indicated marked neutrophil accumulation within the implant, and antibody-specific analysis showed a very low incidence of Chi-specific reactions.[24] It was then described as a relatively inert biomaterial that does not elicit a chronic immune response. The inflammatory response to Alg crosslinked with $CaCl_2$ was previously reported with contradictory conclusions. Some studies described it as a material with high immunogenicity[30] as after 14 days of its implantation fibroblasts began to secrete collagen and macrophages were still present in the tissue.[25] However, in other studies, it has been described as a material with no specific inflammation
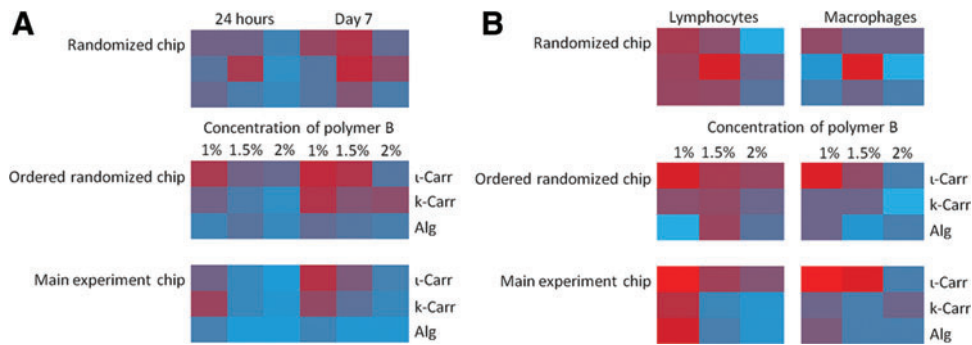
FIG. 8. **(A)** Intensity maps of the scores attributed to histological analysis of the tissue surrounding the implanted control chips with biomaterials in a random configuration, according to Supplementary Table S1. The results obtained according to the configuration of the chip (randomized chip), the same results ordered according to the order of the conventional chips (ordered randomized chip), and the results obtained in the normal chips (main experiment chip), for the same conditions (1% Chi, 24 h of implantation). **(B)** On-chip analysis of the results obtained for lymphocyte analysis (left) and macrophages scores (right) after 24 h of implantation, for 1% Chi conditions. The conditions in ''Randomized chips'' are the ones as indicated in Supplementary Table S1. Color images available online at www.liebertpub.com/tec

or reactive granuloma formation.[31] Carrageenans biocompatibility has been questioned in the literature.[32,33] Carrageenan is used to induce paw edema in the rat and mouse and induces IL-8 production through distinct Bcl10 pathway in normal human colonic epithelial cells.[32,33]

We concluded that the presence of Chi in the combinatorial conditions explored in this approach produces a concentration-dependent effect. Porous Chi scaffolds with concentration of 2% led generally to significantly higher inflammatory responses than the ones with 1% or 1.5% (Supplementary Table S2). However, the major effect observed with Chi scaffolds was not their concentration, but the volume of solution used to process the biomaterials. In the conditions 1.5% + Chi (prepared with 6 μL of Chi, instead of 4 μL, as in other conditions), the amount of polymer B was maintained. Regardless of the type of polymer B added to the Chi scaffold, the 1.5% + Chi condition led to higher inflammatory responses regarding histology analysis. We believe that the increase in inflammation with the volume of Chi solution used to prepare the scaffold would be related with the higher biomaterial surface area exposed to the animal tissue. For this, we consider that the total surface exposure of the scaffolds is a major advantage of the system proposed herein, as it allows studying biomaterial volume-dependent phenomena.

Alg was the polymer present in the studied array of materials that led to lower inflammatory responses. k-Carr led to a slightly higher response, in most conditions, not significantly different from Alg. Such polymers showed concentration-dependent effects on inflammatory response. ι-Carr was the material that showed a higher inflammatory response. This effect was concentration-dependent: 2% Chi was the condition that triggered higher inflammatory responses. This fact, along with the lower inflammatory response observed in k-Carr samples, suggests that the inflammatory response triggered by ι-Carr is related to its higher amount of sulfate groups.

Another interesting feature observed in scaffolds containing ι-Carr in all concentrations was the higher amount of blood vessels present in the tissue sections that surrounded the biomaterial after 7 days of implantation (Fig. 5ii). The

method could be probably extended to studies of crossed effects of inflammation, vascularization, and regeneration of tissues.

Validation of the method

Chips with scaffolds disposed in randomly rearranged positions were prepared (indicated in Supplementary Table S1; on-chip immunocytochemistry images can be seen in Supplementary Figs. S8 and S9). This allowed confirming that the obtained results were not dependent on the relative position of the scaffolds in the chips evidencing the independence of the tissue reaction to the biomaterials with respect to their relative location (Fig. 8A, B), for both histological analysis and immunocytochemistry results.

Implantation of single scaffolds with conventional size was carried out to compare the response observed with the implantation of four chips with distinct biomaterials in a single animal with two randomly chosen conditions. This step of validation of the method consisted in the direct implantation of two distinct biomaterials without using the superhydrophobic platform, with the size of conventionally implanted plugs in tissue engineering field (5 mm diameter × 3 mm height). This was performed in single animals, that is, one plug/animal. Results regarding implantation of biomaterial plugs can be seen in Figure 9. We observed that the adherence of lymphocytes to the scaffold containing ι-Carr was higher and more evenly distributed than to the one containing Alg. Images of histology sections showed that for 24 h of implantation, PMN cells were prevalent around the biomaterial in the Alg-containing scaffolds. For the scaffolds containing ι-Carr, the presence of PMN cells was similar to the Alg-containing scaffolds. However, the presence of lymphocytes was detected around the implanted material (blue arrows for lymphocytes and green arrows indicating the material, Fig. 9). After 7 days of cell culture, in the Alg-containing scaffold, the presence of PMN cells (orange arrows, Fig. 9) was still prevalent. In the scaffold ι-Carr, histology showed macrophages adhered to the biomaterial (black arrows, Fig. 9). These results were consistent with the results observed on-chip, for both on-chip lymphocyte analysis and histology
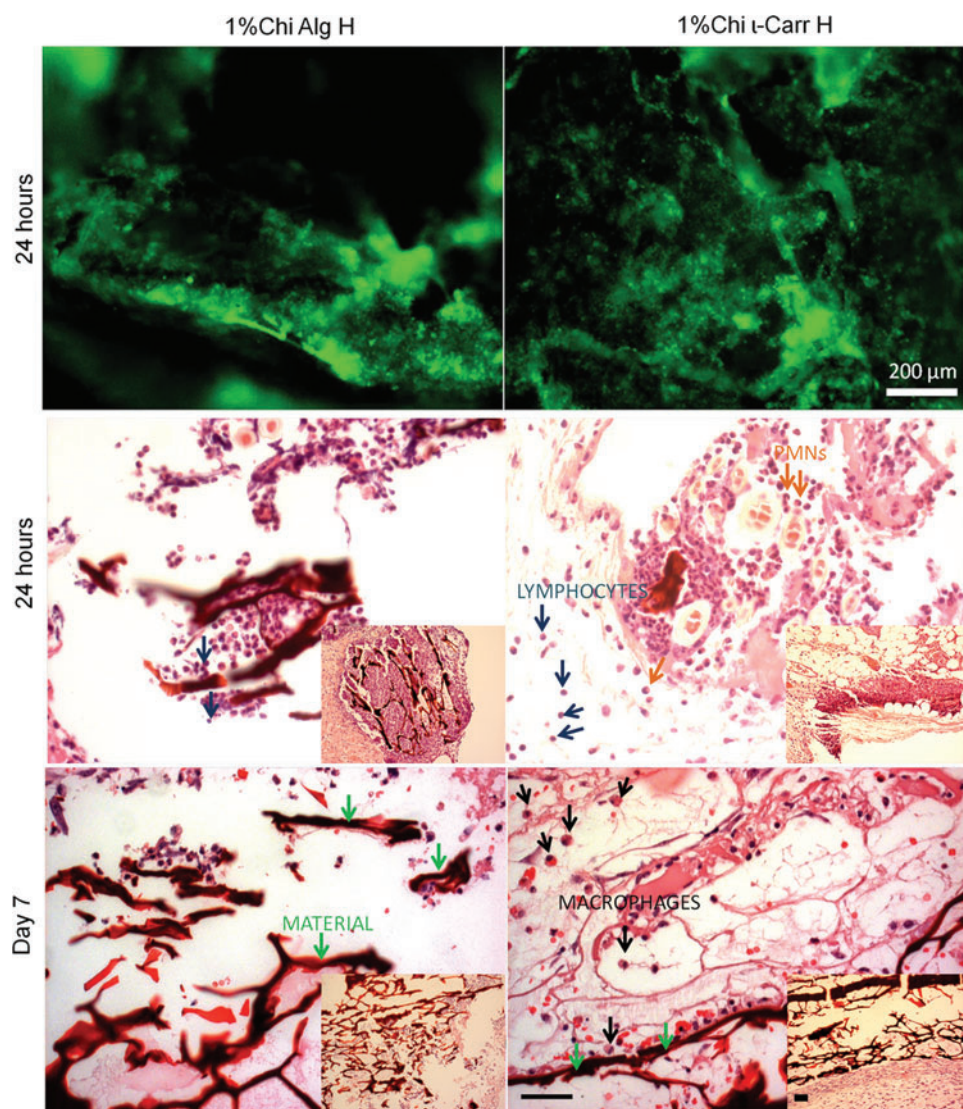
FIG. 9. Results obtained from the analysis of implanted scaffold plugs with conventional sizes (5 mm × 3 mm). Lymphocyte immuno-cytochemistry images (upper line images). Images of histology sections (middle and lower lines images) after 24 h and 7 days of implantation. Blue arrows indicate lymphocytes, and green arrows indicate the biomaterial. PMN cells are indicated with orange arrows and the scaffold is indicated with black arrows, for 7 days images. Scale bars in histological cuts figures = 200 μm. PMN, polymorphonuclear. Color images available online at www.liebertpub.com/tec

analysis. After 24 h of implantation, the amount of lymphocytes detected on-chip was lower for Alg-containing scaffolds compared to the ones with ι-Carr. The amount of macrophages after 24 h of implantation on both conditions studied on-chip was not significantly different. After 7 days of implantation, the amount of macrophages adhered to the scaffolds containing ι-Carr was clearly higher than in the ones containing Alg, as was corroborated by the plugs results. As such, we conclude that the results obtained for on-chip analysis with miniaturized scaffolds were coherent with the implantation of single plugs without the superhydrophobic film.

Polystyrene chips without biomaterials were also implanted in the rats. We verified that general cell adhesion to the superhydrophobic side of the chip was much lower than to the wettable domains on both time points (see DAPI blue staining of cell nuclei). Regarding the adhered cells, we could see that after 24 h of implantation, the lymphocyte adhesion on the wettable spots occurred, whereas in the superhydrophobic domains of the chip was almost totally avoided. After 7 days of implantation, no macrophages were detected in the superhydrophobic domain of the chips (Fig. 10A). Histological analysis (Fig. 10B) showed that inflam-

matory response observed after 24 h (Fig. 10B1) of implantation was very mild. The presence of a low amount of PMN cells was registered very close to the site of implantation. After 7 days of implantation (Fig. 10B2), the inflammatory response seemed to increase slightly around the chips. The cells present around the chip were PMN, along with some lymphocytes and macrophages. Also in the empty chips implanted in one animal along with three chips with biomaterials with the conditions 1% Chi, 1.5% Chi, and 2% Chi, the observed inflammatory response was very mild. After 24 h (Fig. 10C1) of implantation, a low presence of macrophages and PMN cells was observed. After 7 days of implantation (Fig. 10C2), a very low presence of inflammatory cells was registered. This suggests that the water repellence that characterizes these surfaces and its propensity to decrease protein adhesion[29] lowers the tissue response in the superhydrophobic sites. The lower surface contact between the tissue and the materials was previously reported to decrease inflammatory response.[34] Along with the previously described control results, these observations strengthen the idea that the response between patterned biomaterials will be independent of spot to spot in the chip.
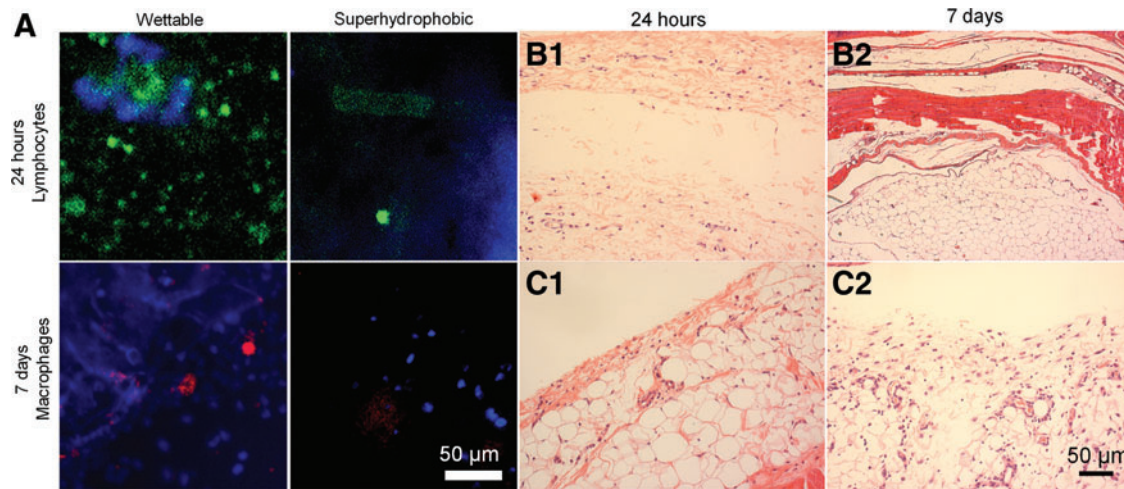
FIG. 10. **(A)** Immunocytochemistry images for lymphocytes (after 24 h of implantation) and macrophages (after 7 days of implantation) of empty chips, without any biomaterials spotted in the wettable regions. Two identical chips were implanted by animal. **(B)** Histological (H&E staining) sections of the tissue surrounding a chip (without any biomaterial spotted in the wettable regions). Two identical chips were implanted by animal. **(C)** Histological (H&E staining) sections of the tissue surrounding empty chips (without any biomaterial spotted in the wettable regions). These chips were implanted along with three chips with biomaterials with the conditions 1% Chi, 1.5% Chi, and 2% Chi, observed after 24 h and 7 days of implantation. H&E, hematoxylin and eosin. Color images available online at www.liebertpub.com/tec

Significance of the method

High-throughput methods are increasing and expanding their areas of application, allowing rapidly answering complex questions in the field of biomaterials. We demonstrated the possibility of performing high-throughput *in vivo* analysis of inflammatory response to distinct biomaterials using affordable superhydrophobic patterned thin and flat surfaces. We validated the method by distributing the arrays of biomaterials randomly and by comparing the results from implanting conventional-size biomaterial plugs in individual animals. This approach allowed studying new combinations of biomaterials and assessing their inflammation-triggering potential. The patterning of biomaterials in the proposed platforms allowed having biomaterials with total surface exposure, to maximize the contact with the *in vivo* environment. We saw that a combined analysis of on-chip and histology observation leads to an accurate evaluation of the materials' performance. Moreover, after 7 days of implantation, the on-chip analysis was correspondent to the histology scores attribution. This may allow, in the future, shortening the time of results analysis, working solely with on-chip results that can be assessed rapidly through direct image analysis. This method allows reducing the number of animals while screening biomaterials for inflammatory response.

This work demonstrated the feasibility of the method by analyzing different combinations of a few polysaccharides, a class of natural materials widely used in biomedical application.[35] These studies could be easily extended to many combinations of other materials and may be complemented with long-term regeneration studies, where the combined effect of inflammation may be beneficial for the vascularization and regeneration of the implants. In such studies, biomaterials that promote an ideal balance of inflammatory cells recruitment to promote tissue regeneration and do not induce the rejection of the biomaterial by the host would be hit-spotted. Biomaterials with distinct shapes and aniso-

tropic features may also be patterned and implanted, and the performance of the materials in both sides of the chips may also be studied to assess the response of distinct tissues in contact with two faces of the film. Moreover, we foresee the development of new chips with distinct flexibility and stiffness. Those would be useful not only as subcutaneous implants but also to be used in other anatomic sites where tissues require adaptation of the shape of the chip, such as cardiac, vascular tissue, or bone.

Conclusion

We demonstrated the application of superhydrophobic chips patterned with wettable regions as implantable platforms for the high-content *in vivo* study of inflammatory response caused by biomaterials. We tested 36 combinations of biomaterials in the form of freeze-dried 3D scaffolds simultaneously in one animal. The integration of the data obtained from the on-chip lymphocyte and macrophage analyses, as well as histological analysis of the surrounding tissue, with control data showed the applicability of these chips as platforms for the rapid screening of *in vivo* biomaterials' response. We believe that in the future such methodology may be applied in distinct approaches regarding, for example, complex multivariable tissue regeneration studies.

Acknowledgments

PTDC/CTM-BIO/1814/2012, Pest-C/SAU/UI0709/2011 and PEst-OE/EGE/UI4056/2011.

Disclosure Statement

No competing financial interests exist.

References

1. Anderson, J.M., Rodriguez, A, and Chang, D.T. Foreign body reaction to biomaterials. Seminar Immunol **20,** 86, 2008.
2. Veriter, S., Mergen, J., Goebbels, R.M., Aouassar, N., Gregoire, C., Jordan, B., Leveque, P., Gallez, B., Gianello, P., and Dufrane, D. In vivo selection of biocompatible alginates for islet encapsulation and subcutaneous transplantation. Tissue Eng Part A **16,**1503, 2010.
3. Mountziaris, P.M., and Mikos, A.G. Modulation of the inflammatory response for enhanced bone tissue regeneration. Tissue Eng Part B Rev **14,** 179, 2008.
4. Kyritsis, N., Kizil, C., Zocher, S., Kroehne, V., Kaslin, J., Freudenreich, D., Iltzsche, A., and Brand, M. Acute inflammation initiates the regenerative response in the adult zebrafish brain. Science **338,** 1353, 2012.
5. Godwin, J.W., Pinto, A.R., and Rosenthal, N.A. Macrophages are required for adult salamander limb regeneration. Proc Natl Acad Sci U S A **110,** 9415, 2013.
6. Liu, Y., Wang, L., Kikuiri, T., Akiyama, K., Chen, C.D., Xu, X.T., Yang, R.L., Chen, W.J., Wang, S.L., and Shi, S.T. Mesenchymal stem cell-based tissue regeneration is governed by recipient T lymphocytes via IFN-gamma and TNF-alpha. Nat Med **17,** 1594, 2011.
7. MacLean, D., and Kamoun, S. Big data in small places. Nat Biotechnol **30,** 33, 2012.
8. Ebert, A.D., and Svendsen, C.N. Human stem cells and drug screening: opportunities and challenges. Nat Rev Drug Discov **9,** 367, 2010.
9. McCoy, J.P. High-content screening: getting more from less. Nat Methods **8,** 390, 2011.
10. Brafman, D.A., Chien, S., and Willert, K. Arrayed cellular microenvironments for identifying culture and differentiation conditions for stem, primary and rare cell populations. Nat Protoc **7,** 703, 2012.
11. Burdick, J.A., and Watt, F.M. High-throughput stem-cell niches. Nat Methods **8,** 915, 2011.
12. Desbordes, S.C., and Studer, L. Adapting human pluripotent stem cells to high-throughput and high-content screening. Nat Protoc **8,** 111, 2013.
13. Gobaa, S., Hoehnel, S., Roccio, M., Negro, A., Kobel, S., and Lutolf, M.P. Artificial niche microarrays for probing single stem cell fate in high throughput. Nat Methods **8,** 949, 2011.
14. Lecault, V., VanInsberghe, M., Sekulovic, S., Knapp, D., Wohrer, S., Bowden, W., Viel, F. McLaughlin, T., Jarandehei, A., Miller, M., Falconnet, D., White, A.K., Kent, D.G., Copley, M.R., Taghipour, F., Eaves, C.J., Humphries, R.K., Piret, J.M., and Hansen, C.L. High-throughput analysis of single hematopoietic stem cell proliferation in microfluidic cell culture arrays. Nat Methods **8,** 581, 2011.
15. Mei, Y., Saha, K., Bogatyrev, S.R., Yang, J., Hook, A.L., Kalcioglu, Z.I., Cho, S.W., Mitalipova, M., Pyzocha, N., Rojas, F., Van Vliet, K.J., Davies, M.C., Alexander, M.R., Langer, R., Jaenisch, R., and Anderson, D.G. Combinatorial development of biomaterials for clonal growth of human pluripotent stem cells. Nat Mater **9,** 768, 2010.
16. Hook, A.L., Chang, C.Y., Yang, J., Luckett, J., Cockayne, A., Atkinson, S., Mei, Y., Bayston, R., Irvine, D.J., Langer, R., Anderson, D.G., Williams, P., Davies, M.C., and Alexander, M.R. Combinatorial discovery of polymers resistant to bacterial attachment. Nat Biotechnol **30,** 868, 2012.
17. Curtarolo, S., Hart, G.L.W., Nardelli, M.B., Mingo, N., Sanvito, S., and Levy, O. The high-throughput highway to computational materials design. Nat Mater **12,** 191, 2013.
18. Song, W.L., Veiga, D.D., Custodio, C.A., and Mano, J.F. Bioinspired degradable substrates with extreme wettability properties. Adv Mater **21,** 1830, 2009.
19. Neto, A.I., Custodio, C.A., Song, W.L., and Mano, J.F. High-throughput evaluation of interactions between biomaterials, proteins and cells using patterned superhydrophobic substrates. Soft Matter **7,** 4147, 2011.
20. Salgado, C.L., Oliveira, M.B., and Mano, J.F. Combinatorial cell-3D biomaterials cytocompatibility screening for tissue engineering using bioinspired superhydrophobic substrates. Integr Biol **4,** 318, 2012.
21. Oliveira, M.B., Salgado, C.L., Song, W.L., and Mano, J.F. Combinatorial on-chip study of miniaturized 3D porous scaffolds using a patterned superhydrophobic platform. Small **9,** 768, 2013.
22. Ballester-Beltran, J., Rico, P., Moratal, D., Song, W.L., Mano, J.F., and Salmeron-Sanchez, M. Role of superhydrophobicity in the biological activity of fibronectin at the cell-material interface. Soft Matter **7,** 10803, 2011.
23. Chang, D., Saidel, G., and Anderson, J. Dynamic systems model for lymphocyte interactions with macrophages at biomaterial surfaces. Cel Mol Bioeng **2,** 573, 2009.
24. Kim, H., Tator, C.H., and Shoichet, M.S. Chitosan implants in the rat spinal cord: Biocompatibility and biodegradation. J Biom Mat Res A **97A,** 395, 2011.
25. Nunamaker, E.A., Purcell, E.K., and Kipke, D.R. *In vivo* stability and biocompatibility of implanted calcium alginate disks. J Biom Mat Res A **83A,** 1128, 2007.
26. Masferrer, J.L., Zweifel, B.S., Manning, P.T., Hauser, S.D., Leahy, K.M., Smith, W.G., Isakson, P.C., and Seibert, K. Selective inhibition of inducible cyclooxygenase 2 *in vivo* is antiinflammatory and nonulcerogenic. Proc Natl Acad Sci U S A **91,** 3228, 1994.
27. Oliveira, N.M., Neto, A.I., Song, W.L., and Mano, J.F. Two-dimensional open microfluidic devices by tuning the wettability on patterned superhydrophobic polymeric surface. Appl Phys Express **3,** 085205, 2010.
28. Chang, D.T., Colton, E., Matsuda, T., and Anderson, J.M. Lymphocyte adhesion and interactions with biomaterial adherent macrophages and foreign body giant cells. J Biom Mat Res A **91A,** 1210, 2009.
29. VandeVord, P.J., Matthew, H.W.T., DeSilva, S.P., Mayton, L., Wu, B., and Wooley, P.H. Evaluation of the biocompatibility of a chitosan scaffold in mice. J Biom Mat Res **59,** 585, 2002.
30. Smidsrød, O., and Skjåk-Braek, G. Alginate as immobilization matrix for cells. Trends Biotech **8,** 71, 1990.
31. Lima, A.C., Batista, P., Valente, T.A.M., Silva, A.S., Correia, I.J., and Mano, J.F. Novel methodology based on biomimetic superhydrophobic substrates to immobilize cells and proteins in hydrogel spheres for applications in bone regeneration. Tissue Eng Part A **19,** 1175, 2013.
32. Morris, C. Carrageenan-induced paw edema in the rat and mouse. In: Winyard, P., and Willoughby, D., eds. Inflammation Protocols. New York, NY: Humana Press, 2003, Vol. 225, pp. 115.
33. Borthakur, A., Bhattacharyya, S., Dudeja, P.K., and Tobacman, J.K. Carrageenan induces interleukin-8 production

through distinct Bcl10 pathway in normal human colonic epithelial cells. Am J Physiol Gastrointest Liver Physiol **292,** G829, 2007.

34. Mahdavi, A., Ferreira, L., Sundback, C., Nichol, J.W., Chan, E.P., Carter, D.J.D., Bettinger, C.J., Patanavanich, S., Chignozha, L., Ben-Joseph, E., Galakatos, A., Pryor, H., Pomerantseva, I., Masiakos, P.T., Faquin, W., Zumbuehl, A., Hong, S., Borenstein, J., Vacanti, J., Langer, R., and Karp, J.M. A biodegradable and biocompatible gecko-inspired tissue adhesive. Proc Natl Acad Sci U S A **105,** 2307, 2008.

35. Mano, J.F., Silva, G.A., Azevedo, H.S., Malafaya, P.B., Sousa, R.A., Silva, S.S., Boesel, L.F., Oliveira, J.M., Santos, T.C., Marques, A.P., Neves, N.M., and Reis, R.L. Two-dimensional open microfluidic devices by tuning the wettability on patterned superhydrophobic polymeric surface. J R Soc Interface **4,** 999, 2007.

Address correspondence to:
João F. Mano, PhD
3B's Research Group—Biomaterials, Biodegradables
and Biomimetics
University of Minho
Headquarters of the European Institute of Excellence
on Tissue Engineering and Regenerative Medicine
AvePark
4806-909 Taipas
Guimarães
Portugal

E-mail: jmano@dep.uminho.pt